Sensors Hot Paper

Human Cyclophilin B Nuclease Activity Revealed via Nucleic Acid-Based Electrochemical Sensors

Vincent Clark, Kelly Waters, Ben Orsburn, Namandjé N. Bumpus, Nandini Kundu, Jonathan T. Sczepanski, Partha Ray,* and Netzahualcóyotl Arroyo-Currás*

Abstract: Human cyclophilin B (CypB) is oversecreted by pancreatic cancer cells, making it a potential biomarker for early-stage disease diagnosis. Our group is motivated to develop aptamer-based assays to measure CypB levels in biofluids. However, human cyclophilins have been postulated to have collateral nuclease activity, which could impede the use of aptamers for CypB detection. To establish if CypB can hydrolyze electrode-bound nucleic acids, we used ultrasensitive electrochemical sensors to measure CypB's hydrolytic activity. Our sensors use ssDNA and dsDNA in the biologically predominant D-DNA form, and in the nuclease resistant L-DNA form. Challenging such sensors with CypB and control proteins, we unequivocally demonstrate that CypB can cleave nucleic acids. To our knowledge, this is the first study to use electrochemical biosensors to reveal the hydrolytic activity of a protein that is not known to be a nuclease. Future development of CypB bioassays will require the use of nuclease-resistant aptamer sequences.

Introduction

Human cyclophilin B (CypB) is a peptidyl-prolyl cis-trans isomerase enzyme ubiquitously found in human tissues that catalyzes the isomerization of proline-imidic peptide bonds to regulate protein folding.[1] Inside cells, CypB localizes in the endoplasmic reticulum.[2] However, the protein also participates in the secretory pathway and is released to biological fluids.[3] CypB maintains mitochondrial functions[4] and plays roles in apoptosis,[2] regulation of T-cell function and inflammation,[5] the pathogenesis of vascular disease,[6] and viral infections.[7,8] CypB is signifi-

cantly overproduced in pancreatic cancer,[2,6,9] making it an attractive diagnostic biomarker for this disease. Specifically, CypB is found at concentrations ≈ 15 nM in the serum of pancreatic cancer patients, versus serum concentrations of ≈ 3 nM for healthy individuals.[6,10,11] A different biomarker, CA 19–9, is currently approved for pancreatic cancer diagnosis. However, this antigen can be produced non-specifically in benign and malignant tumor cells, leading to a high rate of false results.[12] Although other biomarkers are being investigated,[13] CypB is considered a promising candidate to increase the accuracy of positive pancreatic cancer diagnoses.[10] Thus, there is a strong motivation to develop clinically validated assays to measure CypB in patient fluids.

An additional, less investigated function of CypB is its collateral nuclease activity. Prior published works reported the ability of human cyclophilins to hydrolyze both single- and double-stranded nucleic acids.[14] Montague et al. performed solution-phase nuclease assays and concluded that *E. coli*-produced human cyclophilins A, B, and C degrade linear single- and double-stranded plasmid DNA (pUC18) under non-denaturing conditions.[14,15] However, these results were contested by Manteca and Sanchez,[16] who made the argument that the nuclease activity of recombinantly produced cyclophilins is due to the presence of contaminant nucleases from the host organism. Independently, Nagata et al. indicated that CypB may participate in the induction of chromosomal DNA degradation during cell death execution of TCR-stimulated thymocytes.[17] To our knowledge, there are no additional reports regarding the nuclease activity of human cyclophilins. However, given the known relevance of this protein's activity to viral infection, cancer and apoptosis,[2,6–8,18] there remains a critical need to further investigate CypB enzymatic functions that may play key roles in disease physiology. In addition, the use of nucleic

[*] V. Clark, Dr. N. Arroyo-Currás
Chemistry-Biology Interface Program, Zanvyl Krieger School of Arts
& Sciences, Johns Hopkins University
Baltimore, MD 21218 (USA)
E-mail: netzarroyo@jhmi.edu

K. Waters, Dr. B. Orsburn, Dr. N. N. Bumpus, Dr. N. Arroyo-Currás
Department of Pharmacology and Molecular Sciences,
Johns Hopkins University School of Medicine
Baltimore, MD 21205 (USA)

Dr. N. Kundu, Dr. J. T. Sczepanski
Department of Chemistry, Texas A&M University
College Station, Texas, TX 77842 (USA)

Dr. P. Ray
Department of Surgery, Division of Surgical Oncology, Moores
Cancer Center, Department of Medicine, Division of Infectious
Diseases and Global Public Health, University of California San
Diego Health
San Diego, CA 92093 (USA)
E-mail: pray@health.ucsd.edu

acid aptamers against secreted CypB[10] for diagnostic applications could be affected by the protein's collateral nuclease activity.[19] Thus, further investigation of this catalytic activity may be critical to diagnostic assay development.

In this work we investigate the collateral nuclease activity of commercially available human CypB to determine whether aptamer-based sensor development is a feasible approach for CypB monitoring. We followed a two-pronged approach to evaluate CypB's nuclease activity: first, we used ultrasensitive nucleic acid-based electrochemical sensors to confirm that pure, nuclease free CypB can hydrolyze electrode-bound ssDNA, duplex DNA/DNA and DNA/F-RNA hybrids in buffered solutions under physiological conditions of pH and ionic strength. And second, we performed purity and CypB-driven nucleic acid fragmentation analyses using mass spectrometry to demonstrate the absence of any contaminant nucleases remaining from the host human cell expression system. Our results strongly indicate that CypB has intrinsic nuclease activity. To our knowledge, this is the first study to use electrochemical nucleic acid-based sensors to reveal the hydrolytic activity of a protein not previously known to be a nuclease.

Results and Discussion

Our approach to study CypB's nuclease activity uses nucleic acid-based electrochemical sensors (NBEs), a sensitive ex vivo approach to evaluate the nuclease activity of proteins.[19,20] These sensors consist of mixed self-assembled monolayers of alkanethiols and redox reporter- and alkanethiol-modified oligonucleotides, formed on gold electrodes (Figure 1A, top). In NBEs, electron transfer can be measured between the redox reporter and the electrode surface via square wave voltammetry (Figure 1A, bottom). The platform can be used to study nucleic acid hydrolysis via continuous monitoring of the reporter's voltametric signal following protein additions.[19,20] The idea is that if CypB can hydrolyze nucleic acids, addition of this protein to solutions where NBEs are immersed should result in cleavage of the electrode-bound oligos (Figure 1B, top), releasing the reporter-modified strands to the bulk solution where they get infinitely diluted and cannot be detected. This effect is seen as a decrease in the sensor's voltametric currents (Figure 1B, bottom). Because only a finite number of reporter-modified oligonucleotides are bound to the electrode and exhaustively electrolyzed in a voltametric sweep, the approach is sensitive to even small changes in reporter availability caused by nucleic acid cleavage.
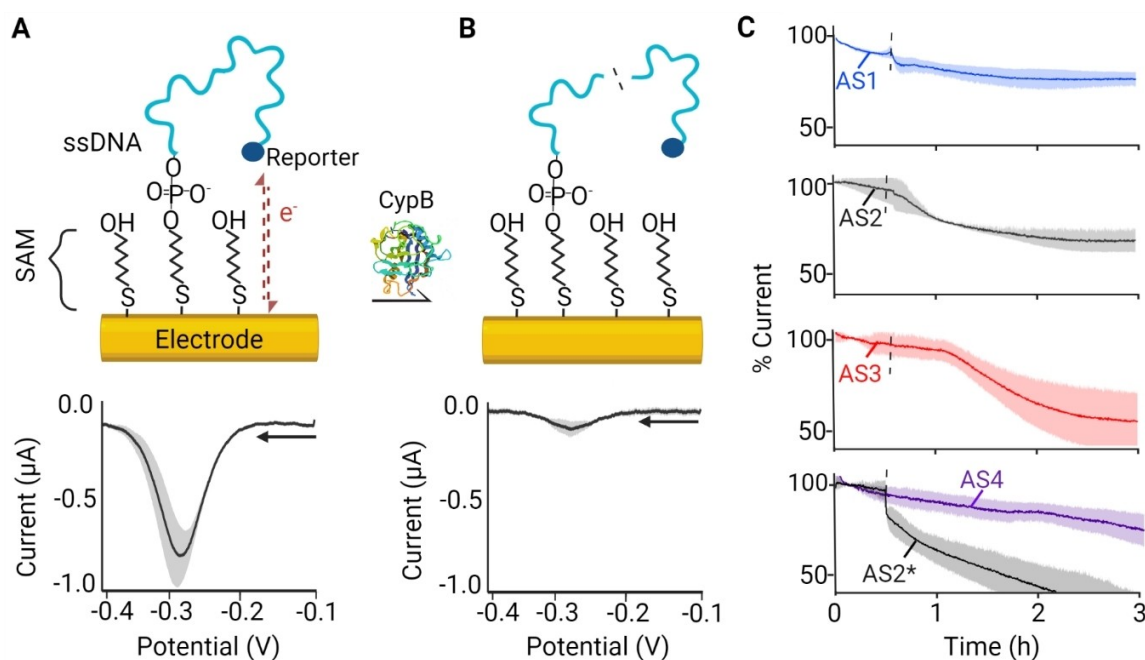
Figure 1. Measurement of nuclease-driven nucleic acid hydrolysis via NBEs. A) The platform consists of a mixed self-assembled monolayer (SAM) of alkanethiols and reporter-, alkanethiol-modified oligonucleotides on gold electrodes. In NBEs, electron transfer can be voltammetrically measured between the reporter (here methylene blue) and the electrode surface. B) Because only a finite number of reporter-modified oligonucleotides are available on the NBE interface (≈ 2 pmol cm^{-2}),[21] protein-driven hydrolysis of any of them leads to a significant loss of voltammetric currents.[19,20] Bottom panels illustrate experimental changes in voltametric currents going from an NBE interface containing only single-stranded DNA ($t = 0$ h), to the same interface after nuclease cleavage ($t = 3$ h). C) Voltammetric peak currents measured every 11 s for NBEs fabricated with sequences AS1, AS2, AS3, and AS4 (Table S1). Dashed lines indicate the moment of CypB addition. All measurements performed by square wave voltammetry in phosphate-buffered saline (pH = 7.4), using a square wave frequency of 250 Hz, amplitude of 25 mV, and potential step of 1 mV. The asterisk indicates the presence of 1 mM Mg^{2+} and 1 mM Ca^{2+} in the buffer. Solid lines represent the average measurement of 4 sensors, shaded areas show their standard deviation. Black arrows indicate the direction of the voltammetric scan.

We first evaluated the ability of CypB to hydrolyze single stranded DNA (ssDNA) in NBEs. We used human CypB recombinantly produced in human embryonic kidney (HEK293) cells from Sino Biological (Catalog number: 11004-H08H). This protein has a molecular weight of ≈22 kDa and consists of 190 amino acids. The protein is sold fused to a signal peptide at the N-terminus and a polyhistidine tag at the C-terminus. The vendor claims a purity >96%, as determined by Coomassie staining of sodium dodecyl sulfate-polyacrylamide gels (SDS-PAGE) following protein resolution. We independently confirmed the purity of the protein via mass spectrometry, as discussed later in this manuscript. To prepare the NBEs, we functionalized freshly cleaned gold electrodes (see Materials and Methods in the Supporting Information file) with ssDNA sequences varying in length and secondary structure (Table S1) and mercaptohexanol to form the electrode blocking monolayer (as in Figure 1A). We voltammetrically interrogated these sensors in phosphate-buffered saline every 11 s for 40 min to establish a baseline, and then challenged them with enough CypB to reach a 500 nM concentration. We monitored changes in voltammetric currents following the protein addition for 2.5 h. Doing so we observed a clear protein-related drop in voltammetric currents (Figure 1C), which we attributed to CypB-driven cleavage of electrode-bound oligonucleotides from the sensor surface.

For NBEs functionalized with ssDNA oligos shorter or equal to 20 nt long, CypB additions caused a modest drop (≈20%) in voltammetric currents (AS1 in Figure 1C). However, for NBEs employing ssDNA longer than 20 nt, the currents dropped by as much as 50% (AS2 and AS3 in Figure 1C). The magnitude of the current loss seemed to be a function of oligonucleotide sequence and secondary structure, with the largest current drop seen for a linear poly-dT sequence (AS3) vs a hairpin-shaped oligo (AS2). The delay in current decay observed when using AS3-functionalized NBEs was reproducible and may be attributed to the known sequence-dependent rate of hydrolysis of ssDNA nucleases.[22]

Like other known ssDNA nucleases, CypB cannot cleave left-handed ssDNA isomers (L-DNA). This is because human nucleases are biologically configured to operate on D-DNA only, making L-DNA nuclease resistant.[23,24] In prior work we demonstrated this effect specifically on the NBE platform using nuclease S1, an endonuclease that selectively hydrolyzes ssDNA but can also hydrolyze single-stranded regions in duplex DNA such as loops or gaps.[20] When challenged with nuclease S1, L-DNA-functionalized NBE currents did not decay. Similarly, in this work NBEs functionalized with L-DNA sequence AS4 (Table S1) did not undergo hydrolytic cleavage by CypB, showing stable voltammetric currents that did not decay more than the natural drift of the sensors (AS4 in Figure 1C). These results strongly indicate that CypB has nuclease activity on ssDNA. This activity can be independent of solvated Ca^{2+} and Mg^{2+}, as reported before,[14] but is enhanced in the presence of both ions at concentrations ≈1 mM (AS2* in Figure 1C).[14]
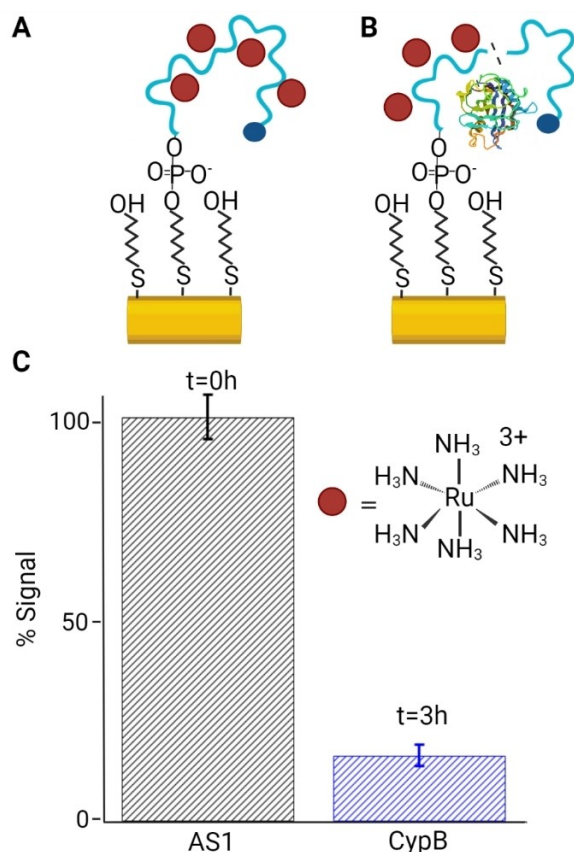
We next evaluated the ability of CypB to hydrolyze double-stranded DNA (dsDNA). For these experiments, we functionalized NBEs with either L-DNA or D-DNA reporter-modified anchor strands (Table S1, sequences AS4 and AS5, respectively). We hybridized the anchor strands with complementary strands of matching nucleic acid stereoisomers to form the DNA duplexes (Figure 2A, sequence C1 from Table S1 in either D- or L- form) in solution prior to monolayer self-assembly. We washed the resulting dsDNA NBEs with phosphate-buffered saline to remove any remaining ssDNA strands. Then, using these sensors in the absence of metallic ion cofactors, we observed no signal decay upon exposure of control dsL-DNA NBEs (Figure 2B, AS4/C1) or dsD-DNA NBEs to 500 nM CypB (Figure 2B, AS5/C1). However, repeating the measurement in phosphate-buffered saline containing 1 mM Ca^{2+} and Mg^{2+} we observed a clear decay of voltammetric currents caused by the addition of CypB (Figure 2B, AS5/C1*). These results match the observations made by Montague et al. and confirm that CypB can hydrolyze both ssDNA and dsDNA in the presence of metallic ion cofactors.[14] In addition, the protein has some nuclease activity on ssDNA in the absence of cofactors as shown in Figure 1C. Such an activity is also seen in homogeneous solution phase via Fluorescence Resonance Energy Transfer (FRET) based assays (Figure S1).

To further demonstrate that the loss of DNA from NBE surfaces is due to strand cleavage by CypB and not sensor drift, we performed quantitative measurements of surface DNA concentration using the method reported by
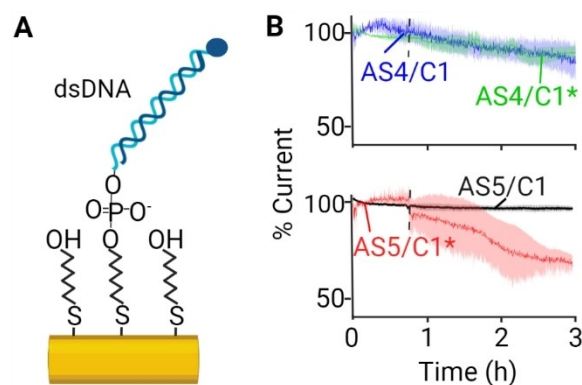
Figure 2. CypB requires Ca^{2+} and Mg^{2+} cofactors to hydrolyze dsDNA. A) NBEs functionalized with dsDNA. The anchor strand (binding to the gold electrode) was functionalized with the reporter methylene blue. The complement strand was added in solution prior to formation of the self-assembled monolayer. The sensors were washed with phosphate-buffer saline prior to testing against CypB. B) All traces represent the voltametric peak current from freshly fabricated NBE sensors using sequences AS4/C1 and AS5/C1 (Table S1) during continuous interrogation. Each trace includes ≈1000 voltametric measurements serially performed every 11 s. Measurements performed in phosphate-buffered saline (pH = 7.4), using a CypB concentration of 500 nM, via square wave voltammetry at a frequency of 250 Hz, amplitude of 25 mV, and potential step of 1 mV. Solid lines represent the average measurement of 3 sensors, and shaded areas show the standard deviation between measurements.

Steel, Herne and Tarlov.[25] The method consists of reacting sensor-bound DNA strands with a low ionic strength buffered solution of ruthenium hexamine, a positively charged complex that binds to the negatively charged DNA backbone. Doing so, the amount of ruthenium hexamine molecules measured by chronocoulometry is directly proportional to the number of phosphate groups present at the sensor surface, providing a direct quantitation of DNA concentration. Using this method on ssDNA NBEs at $t=0$ before addition of 500 nM CypB (Figure 3A), and $t=2$ h after protein addition (Figure 3B, same period as in Figures 1 and 2), we observed a loss of $\approx 80\%$ phosphate groups from the sensor surfaces (Figure 3C). This loss was
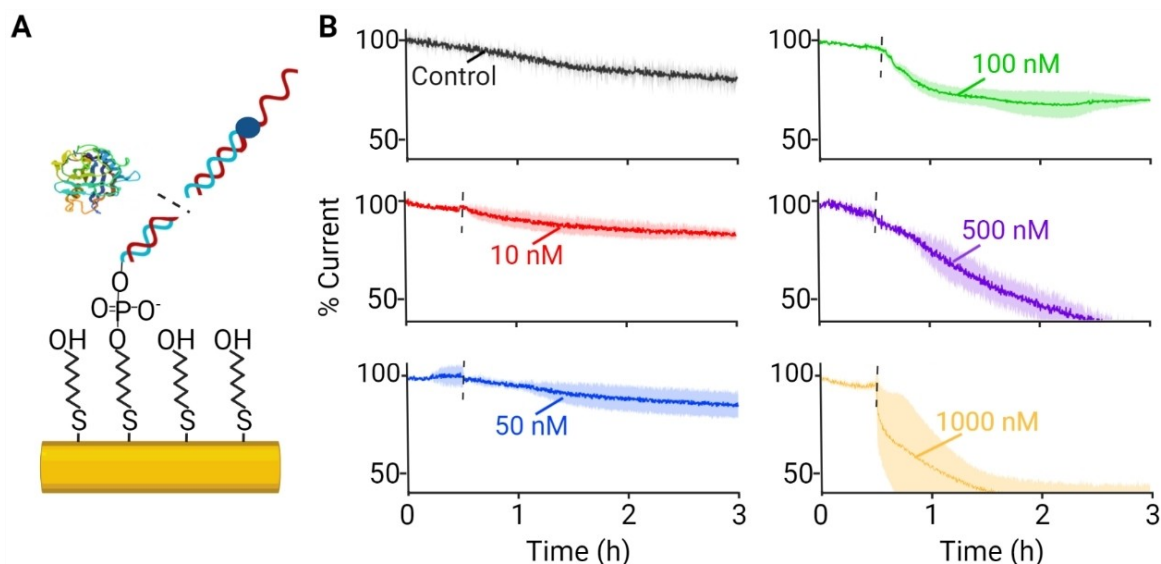
larger than the loss seen from baseline sensor drift (Figure S2).

A nuclease-resistant F-RNA (2′ fluoro-pyrimidine-modified RNA) aptamer binding CypB with a dissociation constant $K_D = 1.5$ nM was previously reported.[10] Seeking to evaluate if this aptamer could be used for CypB bioassays, we used it to functionalize NBEs. Because the CypB F-RNA aptamer was produced via in vitro transcription as reported before,[10] the sequence was not amenable to direct modification with alkylthiol and methylene blue as required for NBE sensing. Instead, we hybridized it to anchor strand AS1 to create DNA/F-RNA hybrid duplexes (AS1/C2, Table S1, Figure 4A). After challenging the resulting NBEs with CypB molar concentrations of 10, 50, 100, 500 and 1000 nM (Figure 4B), we observed that CypB's nuclease activity is concentration dependent. Specifically, at CypB concentrations ≤ 50 nM, the NBEs did not display statistically significant current changes upon protein addition relative to a negative control with no protein additions. However, as we challenged the NBEs with CypB concentrations >50 nM, we observed irreversible decay of NBE currents, as previously seen with ssDNA and dsDNA. The extent of hydrolysis also increased in the presence of metallic ion cofactors (Figure S4).
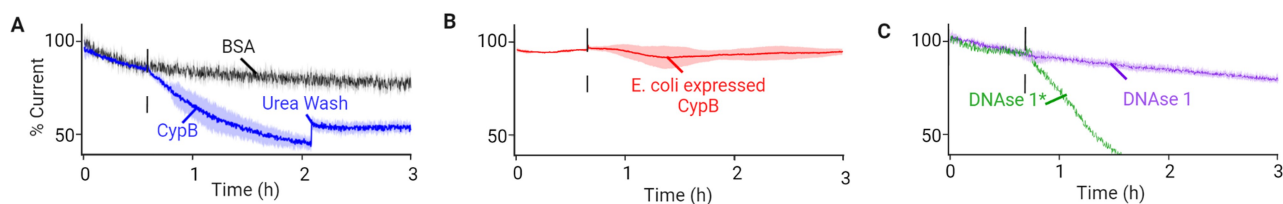
Challenging NBEs with 500 nM of a control protein, bovine serum albumin (BSA), which has no nuclease activity but can strongly and non-specifically bind to sensor surfaces, resulted in no significant current change relative to natural sensor drift (Figure 5A). To further demonstrate that CypB-induced signal decay was not due to sensor fouling, we treated hybrid NBEs with a 30 min-long, 8 M urea wash, two hours after addition of CypB. Urea is a chemical denaturant able to wash non-specifically bound proteins off sensor surfaces.[26] Washing our NBEs with urea did not achieve full signal recovery (Figure 5A), indicating that the oligo-bound redox reporters are irreversibly lost from NBE surfaces upon addition of CypB. These results point to hydrolysis-driven NBE current decay by CypB, instead of simple fouling by non-specific CypB adsorption to the sensor surface.

As an additional control for nuclease activity, we challenged DNA/F-RNA-functionalized NBEs with 500 nM of *E. coli*-produced recombinant human CypB (purchased from Prospec #ENZ-313). This protein is known to undergo post-translational modifications in *E. coli*, specifically acetylation(s) of its lysine residues.[11] Interestingly, the protein lacked nuclease activity as confirmed using our NBE measurements (Figure 5B), indicating that the post-translational modifications in bacteria eliminated the protein's collateral nuclease activity. This observation confirms the claim by Manteca and Sanchez[16] that *E. coli*-produced CypB does not have intrinsic nuclease activity. Nuclease hydrolysis is only observed with CypB produced in human cells.

Seeking to present data corresponding to a positive control, we evaluated the effect of deoxyribonuclease I (DNAse I) on NBEs. DNAse I is an endonuclease that can cleave ssDNA and dsDNA to yield 5′-phosphate mono-

Figure 3. Quantification of surface DNA concentration on NBEs before and after CypB additions. The surface concentration of DNA can be determined by incubating NBEs in buffered solutions of ruthenium hexamine at low ionic strength. A) This redox molecule is positively charged and electrostatically binds to the negatively charged backbone of DNA in direct proportion to the number of phosphate groups present. B) Cleavage of DNA strands results in removal of ruthenium hexamine molecules from the surface. C) Percentage of ruthenium hexamine molecules measured via chronocoulometry (Figure S3) for freshly fabricated NBEs prior to CypB additions, and for NBEs treated with 500 nM CypB. The wait time prior to DNA quantification was 2 h after the protein addition, matching the experimental procedures in Figures 1 and 2. The bars correspond to the normalized, average DNA concentration of 3 sensors, and error boxes to their standard deviation. The absolute surface concentration of DNA was 19 ± 1 picomoles cm^{-2} for control NBEs, and 3.1 ± 0.5 picomoles/cm^2 for CypB-treated NBEs.

Angew. Chem. Int. Ed. **2022**, *61*, e202211292 (4 of 8)

© 2022 The Authors. Angewandte Chemie International Edition published by Wiley-VCH GmbH

Figure 4. CypB-driven hydrolysis of DNA/F-RNA sensors. A) Hybrid DNA/F-RNA sensors via hybridization of a CypB binding F-RNA aptamer to methylene blue- and alkylthiol-modified anchor strands (sequences AS1 and C2 in Table S1, respectively). B) Voltammetric peak currents over time, before and after addition of different concentrations of CypB. Each trace includes ≈1000 voltametric measurements serially performed every 11 s. All measurements were performed using freshly made NBEs immersed in phosphate-buffered saline (pH = 7.4), using a square wave frequency of 250 Hz, amplitude of 25 mV, and potential step of 1 mV. Solid lines represent the average measurement of 3 sensors, and shaded areas show the standard deviation between measurements.


Figure 5. Effect of control proteins on NBE signal decay. A) Effect of challenging DNA/F-RNA (AS1/C2) sensors with 500 nM bovine serum albumin (BSA) on signal decay (black trace). Also shown is a challenge of NBEs with 500 nM CypB, followed by a 30 min-long incubation in 8 M urea (blue trace) to remove any non-specifically bound protein. B) Signal decay controls using 500 nM *E. coli*-expressed CypB. C) Effects of known nuclease DNAse 1 on AS1/C2 hybrids in the absence (purple trace) and presence of metal ion cofactors (green trace). The asterisk indicates the presence of metal cofactors in solution. All measurements were performed using freshly made NBEs immersed in phosphate-buffered saline (pH = 7.4), using a square wave frequency of 250 Hz, amplitude of 25 mV, and potential step of 1 mV. Solid lines represent the average measurement of 3 sensors, and shaded areas show the standard deviation between measurements.

nucleotides and oligonucleotides in the presence of Mg^{2+} ions.[27] Challenging our NBEs with DNAse I in phosphate-buffered saline containing 1 mM Mg^{2+} resulted in an immediate drop of voltammetric currents, indicating cleavage of the anchor AS1 strands (DNAse 1*/AS1/C2* in Figure 5C). In the absence of the metallic ion cofactor, we observed no enzymatic activity (DNAse1/AS1/C2 in Figure 5C). Comparing Figures 4B and 5C shows that, at a molar concentration of 500 nM, CypB cleaves DNA/F-RNA duplexes with similar efficiency to DNAse I.

To address concerns of protein purity and nuclease contamination in our assays, we performed intact mass analysis of our CypB batch using two methods previously reported by Yang et al.[28] and Doneanu et al.[29] Our LC-MS instrument is equipped with an Orbitrap mass analyzer. In orbitrap mass spectrometry, an increase in protein signal can be obtained by using a lower relative resolution, with

the downside of an increase in spurious protein detections. When utilizing lower resolution mass spectrometry, 98.08% of the total LCMS signal corresponded to the estimated mass of CypB (Figure 6A,B). In addition, when using higher resolution mass spectrometry, 88.49% of the total signal corresponded to the mass of CypB, while 7.85% corresponded to the mass of CypB with a single acetylation, and 3.66% of the remaining signal corresponded to 13 ions with masses below 8 kDa (Figure S5), not big enough to indicate the presence of spurious nucleases but, instead, likely the result of in-source CypB decay. Overall, these results point to a high purity sample with no significant amounts of contaminant nucleases.

To determine if CypB can cleave our F-RNA aptamer in addition to the ssDNA anchors from Figure 1 (sequences C2 and AS1 in Table S1), we prepared three samples for tandem mass analysis by mass spectrometry. Sample 1
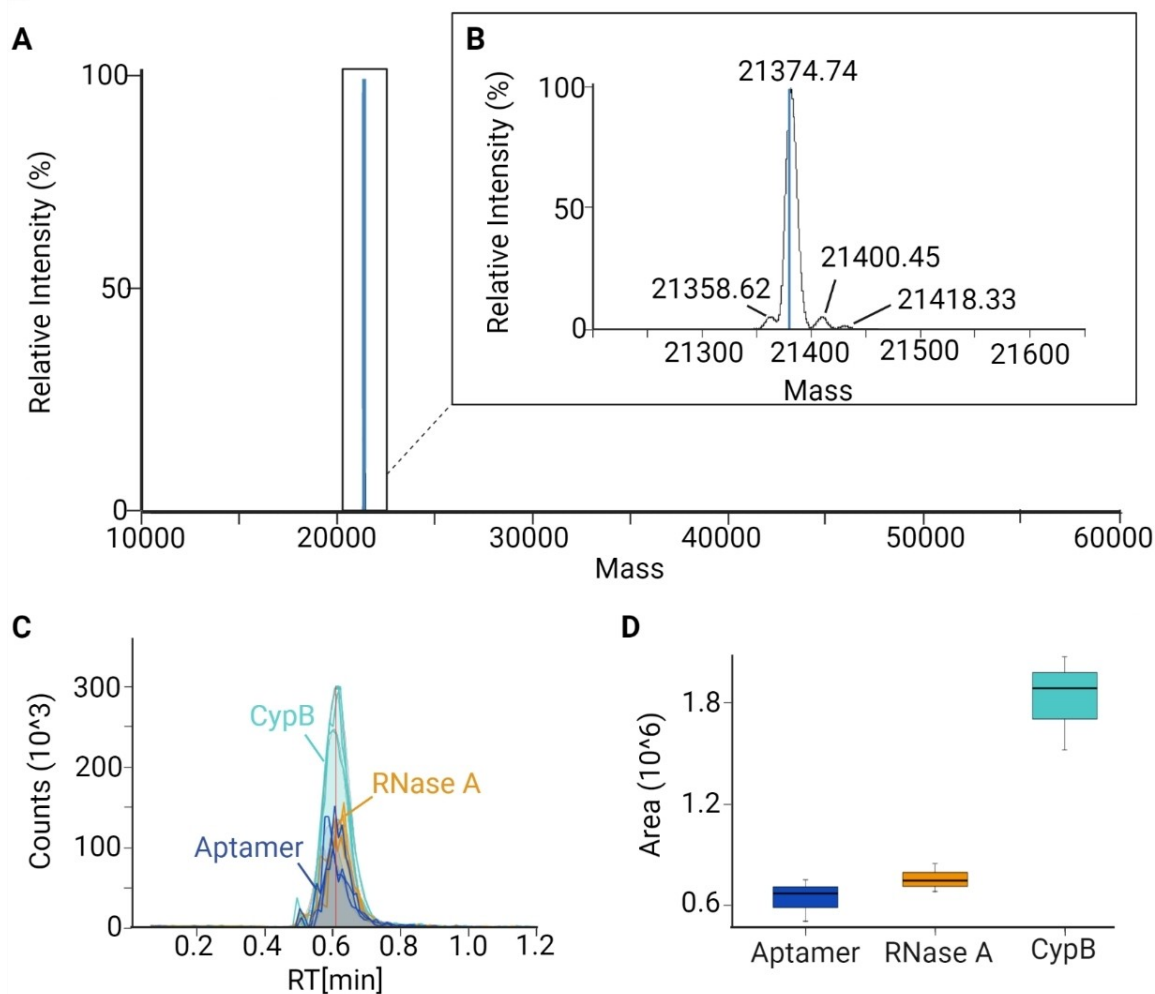
Figure 6. Liquid-chromatography, mass spectrometry analysis of CypB purity. A) 98.08% of protein signal was reported at a molecular mass of 21374.74, which coincides with the molecular mass of the recombinant human CypB used in this study. B) Remaining protein signal corresponds to small populations ±40 mw or 0.18% from the observed mass. C) Extracted ion chromatogram of a nucleotide related compound with an observed molecular weight of 537.79455, with a similarity match of 62.4% to D-ribose-1-phosphate, Δmass of 307.7754. D) The areas under the curve from the extraction ion chromatograph demonstrating greater than three-fold up-increase of the nucleotide fragment following reaction with CypB.

contained the F-RNA aptamer alone (sequence C2 in Table S1). Sample 2 contained the aptamer co-incubated with 500 nM RNase A (control). And Sample 3 contained the aptamer co-incubated with 500 nM CypB. The samples were prepared in phosphate-buffered saline like all the electrochemical measurements and allowed to rest for 3 h. They were then analyzed by mass spectrometry via an untargeted metabolomics approach using a HyperSil Gold C-18 column with a 20 min LC-MS gradient. Three replicates of each sample were performed and compared against the mzCloud database for similarity in oligonucleotide fragmentation. The search identified 31 compounds with similarity score of greater than 60% to D-ribose-1-phosphate with a Δmass ranging from 170.11 Da to 636.92 Da. Among these smaller compounds, 6 were found at a two-fold increased abundance in Sample 2 (C2+RNAse) compared to our control Sample 1 (C2 alone),

while Sample 3 (C2+CypB) displayed a three-fold increase in abundance for 11 fragments relative to Sample 1. Figure 6C displays an example chromatogram for one of such fragments, and Figure 6D the integrated areas under the curve for the same fragment corresponding to each of the three samples. These results indicate higher abundance of small RNA fragments when in the presence of CypB, further indicating that the protein can hydrolyze the F-RNA aptamer in spite of the 2′ fluoro modification of the pentose ring. As a note, we highlight the fact that the purines in the F-RNA aptamer are not fluorinated; therefore, cleavage at purine sites is still possible as indicated by the mass spectrometry measurements.

To evaluate if the nuclease activity of CypB is sufficient to elicit a statistically significant effect on DNA/F-RNA-functionalized NBEs in biofluids, we performed measurements in cell media of a reengineered cell line that

oversecretes CypB in the presence of doxycycline (KPC, Figure S6).[30,31] We also performed additional measurements in cell media of two control cell lines that do not secrete CypB (HEK, GIST-T1) and two cell lines that naturally secrete CypB (Panc-1, MiaPaCa-2, Figure S7). However, given that cell media contains many other proteins in addition to CypB, we observed no statistically significant differences in sensor responses across media from the different cell lines. In more detail, proteins non-specifically adsorbed onto the sensors and sterically pushed methylene blue reporters closer to their surface, temporarily increasing peak currents (Figure S7, first 30 min of data in all graphs). However, the sensors degraded in parallel via previously reported voltage-induced decay mechanisms,[26,32] making peak currents drop after a maximum observed at $\approx t = 30$ min. These results highlight the importance of developing a CypB sensor that relies on affinity interactions for protein detection and not on the reactivity of CypB itself.

Conclusion

We have studied the effects of CypB exposure on the signaling lifetime of nucleic acid-based sensors. Our results unequivocally indicate that CypB acts as a nuclease at supra physiological concentrations (> 50 nM). Previous groups have debated CypB's nuclease activity beginning in 1997 with Montague and colleagues[14] and continuing through the early 2000s with Manteca and Sanchez.[16] Through our two-pronged approach encompassing highly sensitive nucleic acid-based electrochemical assays and mass spectrometry, here we demonstrate that $\geq 98\%$ pure recombinant human CypB has nuclease activity against single stranded and double stranded DNA, as well as against F-RNA. In addition, our results demonstrate that the nuclease activity of CypB can be avoided by employing left-handed stereoisomers of DNA, paving the way for future development of aptamer-based bioassays against this potentially useful biomarker of pancreatic cancer. Although antibodies against CypB (e.g., from Abcam, PN: ab16045) are an additional alternative to the use of aptamers for this application, nucleic acid-based sensors do not require the sample processing nor dilution steps for target detection that antibody-based assays do;[33] therefore, the development of aptamer-based sensors for CypB screening represents an ideal path for rapid diagnostic applications in the clinic.

We note that nucleic acid-based electrochemical sensors were developed originally by Plaxco and colleagues,[34] and have been used to measure the hydrolytic activity of known nucleases.[19,20] Similar, peptide-based sensor platforms have been used to measure the proteolytic activity of known proteases.[35–38] However, this is the first study to report the use of nucleic acid-based electrochemical sensors for the characterization of the hydrolytic activity of a protein that was not previously known to be a nuclease, CypB. As such, the methodologies reported in this work can serve as a future strategy to evaluate nuclease activity of cyclophilins or other proteins suspected to act as nucleases.

Conflict of Interest

The authors declare no conflict of interest.

Data Availability Statement

The data that support the findings of this study are available from the corresponding author upon reasonable request.

[1] J. C. Marini, W. A. Cabral, in *Osteogenesis Imperfecta: Genetics of Bone Biology and Skeletal Disease*, 2nd ed. (Eds.: R. V. Thakker, J. A. Eisman, M. P. Whyte, T. Igarashi), Academic Press, San Diego, **2018**, pp. 397–420.

[2] K. Kim, H. Kim, K. Jeong, M. H. Jung, B.-S. Hahn, K.-S. Yoon, B. K. Jin, G.-H. Jahng, I. Kang, J. Ha, W. Choe, *Apoptosis* **2012**, *17*, 784–796.

[3] E. R. Price, M. Jin, D. Lim, S. Pati, C. T. Walsh, F. D. McKeon, *Proc. Natl. Acad. Sci. USA* **1994**, *91*, 3931–3935.

[4] P. Stocki, D. C. Chapman, L. A. Beach, D. B. Williams, *J. Biol. Chem.* **2014**, *289*, 23086–23096.

[5] A. Denys, F. Allain, B. Foxwell, G. Spik, *Immunology* **1997**, *91*, 609–617.

[6] H. Zhang, Q. Fan, H. Xie, L. Lu, R. Tao, F. Wang, J. Xi, J. Hu, Q. Chen, W. Shen, R. Zhang, X. Yan, *Front Endocrinol* **2017**, *8*, 360.

[7] J. DeBoer, C. J. Madson, M. Belshan, *Virology* **2016**, *489*, 282–291.

[8] K. Watashi, N. Ishii, M. Hijikata, D. Inoue, T. Murata, Y. Miyanari, K. Shimotohno, *Mol. Cell* **2005**, *19*, 111–122.

[9] D. Q. Meng, P. L. Li, M. Xie, *GMR Genet. Mol. Res.* **2015**, *14*, 5346–5354.

[10] P. Ray, K. L. Rialon-Guevara, E. Veras, B. A. Sullenger, R. R. White, *J. Clin. Invest.* **2012**, *122*, 1734–1741.

[11] P. Ray, B. A. Sullenger, R. R. White, *Nucleic Acid Ther.* **2013**, *23*, 435–442.

[12] U. K. Ballehaninna, R. S. Chamberlain, *J. Gastrointest. Oncol.* **2012**, *3*, 105–119.

[13] S. Hasan, R. Jacob, U. Manne, R. Paluri, *Oncol. Rev.* **2019**, *13*, 410.

[14] J. W. Montague, F. M. Hughes, J. A. Cidlowski, *J. Biol. Chem.* **1997**, *272*, 6677–6684.

[15] H. Schneider, N. Charara, R. Schmitz, S. Wehrli, V. Mikol, M. G. M. Zurini, V. F. J. Quesniaux, N. R. Movva, *Biochemistry* **1994**, *33*, 8218–8224.

[16] A. Manteca, J. Sanchez, *J. Bacteriol.* **2004**, *186*, 6325–6326.

[17] T. Nagata, H. Kishi, Q. L. Liu, T. Yoshino, T. Matsuda, Z. X. Jin, K. Murayama, K. Tsukada, A. Muraguchi, *J. Immunol.* **2000**, *165*, 4281–4289.

[18] Q. Wang, B. Xu, K. Fan, J. Wu, T. Wang, *Mediators Inflammation* **2020**, *29*, 6473858.

[19] C. Li, X. Chen, N. Wang, B. Zhang, *RSC Adv.* **2017**, *7*, 21666–21670.

[20] A. Shaver, N. Kundu, B. E. Young, P. A. Vieira, J. T. Sczepanski, N. Arroyo-Currás, *Langmuir* **2021**, *37*, 5213–5221.

[21] N. Arroyo-Currás, K. Scida, K. L. Ploense, T. E. Kippin, K. W. Plaxco, *Anal. Chem.* **2017**, *89*, 12185–12191.

[22] N. A. Desai, V. Shankar, *FEMS Microbiol. Rev.* **2003**, *26*, 457–491.

[23] S. Dey, J. T. Sczepanski, *Nucleic Acids Res.* **2020**, *48*, 1669–1680.

[24] K. P. Williams, X. H. Liu, T. N. Schumacher, H. Y. Lin, D. A. Ausiello, P. S. Kim, D. P. Bartel, *Proc. Natl. Acad. Sci. USA* **1997**, *94*, 11285–11290.

[25] A. B. Steel, T. M. Herne, M. J. Tarlov, *Anal. Chem.* **1998**, *70*, 4670–4677.

[26] K. K. Leung, A. M. Downs, G. Ortega, M. Kurnik, K. W. Plaxco, *ACS Sens.* **2021**, *6*, 3340–3347.

[27] S. Vanecko, M. Laskowski, *J. Biol. Chem.* **1961**, *236*, 3312–3316.

[28] K. Yang, Y. Zhang, R. Chou, L. Yeung, S. Letarte, R.-S. Yang, X. Li, M. Beaumont, R. Gunawan, D. Richardson, S. Dellatore, E. Woolf, Y. Xu, *ACS Pharmacol. Transl. Sci.* **2020**, *3*, 1310–1317.

[29] C. E. Doneanu, M. Anderson, B. J. Williams, M. A. Lauber, A. Chakraborty, W. Chen, *Anal. Chem.* **2015**, *87*, 10283–10291.

[30] S. R. Hingorani, L. Wang, A. S. Multani, C. Combs, T. B. Deramaudt, R. H. Hruban, A. K. Rustgi, S. Chang, D. A. Tuveson, *Cancer Cell* **2005**, *7*, 469–483.

[31] E. Kowarz, D. Löscher, R. Marschalek, *Biotechnol. J.* **2015**, *10*, 647–653.

[32] M. A. Pellitero, S. D. Curtis, N. Arroyo-Currás, *ACS Sens.* **2021**, *6*, 1199–1207.

[33] C. Parolo, A. S. Greenwood, N. E. Ogden, D. Kang, C. Hawes, G. Ortega, N. Arroyo-Currás, K. W. Plaxco, *Microsyst. Nanoeng.* **2020**, *6*, 13.

[34] Y. Xiao, R. Y. Lai, K. W. Plaxco, *Nat. Protoc.* **2007**, *2*, 2875–2880.

[35] E. González-Fernández, N. Avlonitis, A. F. Murray, A. R. Mount, M. Bradley, *Biosens. Bioelectron.* **2016**, *84*, 82–88.

[36] E. González-Fernández, M. Staderini, N. Avlonitis, A. F. Murray, A. R. Mount, M. Bradley, *Sens. Actuators B* **2018**, *255*, 3040–3046.

[37] D.-S. Shin, Y. Liu, Y. Gao, T. Kwa, Z. Matharu, A. Revzin, *Anal. Chem.* **2013**, *85*, 220–227.

[38] Y. Lin, R. Shen, N. Liu, H. Yi, H. Dai, J. Lin, *Anal. Chim. Acta* **2018**, *1035*, 175–183.